Rapid and Facile Detection of PBTC Antiscalant Using Functionalized Polystyrene Nanoparticles and Latex Agglutination

Jirawan Jindakaew, Chariya Kaewsaneha, Chalita Ratanatawanate, Noureddine Lebaz, Patcharapan Suwannin, Nadia Zine, Pakorn Opaprakasit, Abdelhamid Elaissari

Rapid and Facile Detection of PBTC Antiscalant Using Functionalized Polystyrene Nanoparticles and Latex Agglutination

Jirawan Jindakaew[1,2], Chariya Kaewsaneha[2], Chalita Ratanatawanate[3], Noureddine Lebaz[4], Patcharapan Suwannin[1], Nadia Zine[1], Pakorn Opaprakasit[2*], Abdelhamid Elaissari[1]

[1] Universite Claude Bernard Lyon-1, CNRS, ISA-UMR 5280, 69622 Villeurbanne, France

[2] School of Integrated Science and Innovation, Sirindhorn International Institute of Technology (SIIT), Thammasat University, Pathum Thani 12121, Thailand

[3] Environmental Nanotechnology Research Team, Nanohybrids and Coating Research Group, National Nanotechnology Center, National Science and Technology Development Agency, Pathum Thani 12120, Thailand

[4] Universite Claude Bernard Lyon-1, CNRS, LAGEPP-UMR 5007, 69100, Villeurbanne, France

*Corresponding author: pakorn@siit.tu.ac.th (+66 2986 9009 ext 1806)

Abstract

Organophosphate-based compounds, particularly 2-phosphonobutane-1,2,4-tricarboxylic acid (PBTC), have played a crucial role in circulating cooling systems and wastewater treatments as corrosion inhibitors preventing scale deposits in industrial facilities. Employing the reagent within its optimum concentration range is essential for effective performance, minimizing costs and environmental impacts. However, measuring PBTC separately can be challenging due to its functional groups' similarity to other common molecules found in natural water, necessitating complex procedures. In this study, amine-functionalized polystyrene (PS) latex nanoparticles were synthesized through emulsifier-free emulsion polymerization and utilized as nanosorbents for PBTC detection via a straightforward latex agglutination method. This phenomenon is facilitated by electrostatic and hydrogen bonding interactions between the positively charged layers on the particle's surface and the negatively charged PBTC molecules. The pH and concentration of the PBTC solution are key factors influencing the adsorption behaviour and capacity of the functionalized latex particles. A graphical representation of aggregation domains, dependent on both PBTC concentration and pH, was created. This map serves as an effective tool for detecting PBTC concentration. The resulting particles show great promise for monitoring

the concentration range of phosphate additives in water, offering a simple, rapid detection process with low costs and reduced chemical and equipment requirements.

Keywords: PBTC, Latex agglutination, Cationic particles, Polystyrene, Phosphate detection

Graphical abstract

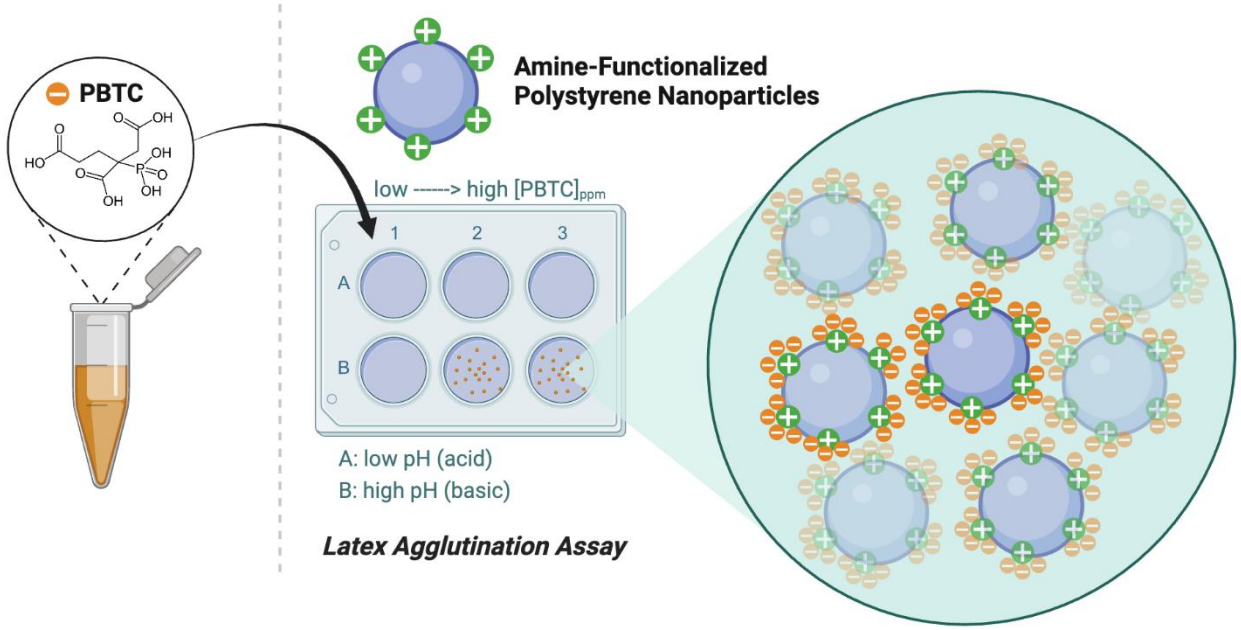

1. Introduction

Scale formation poses a significant challenge in industrial processes. To address this issue, antiscalant agents are employed to inhibit scale formation. Among these, 2-phosphonobutane-1,2,4-tricarboxylic acid (PBTC) is a crucial organophosphate reagent widely used in industrial processes, particularly in circulating cooling water systems. This compound effectively prevents mineral scale formation and corrosion [1-4]. PBTC contains carboxylic and phosphonic acid groups, providing high solubility and strong binding capabilities with various metal ions [5-7]. The fast and accurate monitoring of PBTC concentration during operations and corresponding wastewater treatment processes is essential [8, 9]. In cooling water applications, continuous addition of PBTC is necessary to maintain its optimal concentration and prevent scale formation and corrosion in pipelines and manufacturing equipment [10]. Inadequate organophosphate content in the cooling system can lead to corrosion and scale accumulation during operations. Conversely, an excessive phosphate presence results in higher operating costs and challenges in wastewater treatment. Improper treatments before discharging can degrade water quality and contribute to eutrophication in water resources [11-13]. In aquatic ecosystems, elevated levels of dissolved nutrients can lead to the accelerated growth of water plants or algae blooms, directly affecting surface water conditions and reducing dissolved oxygen levels in water bodies [14, 15].

Detecting the presence of phosphate in a water-cooling system is challenging using conventional spectrophotometric methods because phosphate lacks both fluorescence groups and chromophores. Consequently, it becomes necessary to convert phosphate into free phosphorus, which can then be quantified through optical emission microscopy or a colorimetric method with a reasonable degree of accuracy [16-18]. However, this approach is time-consuming, expensive, and involves intricate processes, the use of toxic chemicals, and costly instruments [19, 20]. Therefore, there is a growing interest in developing novel materials and eco-friendly methods that offer swift responses, enabling time-efficient, accurate monitoring of phosphate in industrial settings at a lower cost.

Adsorption is a promising technology for phosphate removal, demonstrating favourable performance across a wide range of pH values. It offers ease of operation, rapid capture capabilities, cost-effectiveness, a high removal rate for highly toxic pollutants, and generates low levels of harmful secondary products [21-25]. The interaction between compounds and

adsorbents varies depending on environmental factors, including the nature of the adsorbent surface, the pH of the medium, surface charge density, incubation time and temperature, solvent polarity, and the presence of competing molecules [26-28]. Numerous natural silica-based adsorbents, such as zeolites, diatomite, clays, and porous silica materials, have proven effective for phosphate removal. However, raw silica materials lack functional groups or adsorption sites for phosphate adsorption [29]. Modified adsorbents with functional groups have enhanced adsorptive removal efficiency, typically measured in terms of selectivity for specific compounds, adsorption capacity, renewability, and durability. A range of surface functionalization techniques can be employed to improve various surface properties, including hydrophilicity, electrostatic interaction, surface energy, roughness, and biocompatibility [30, 31]. Recently, we developed carboxylated magnetic polymeric nanoparticles (MPNPs) as nanosorbents for the removal of calcium ions (Ca^{2+}) [32]. The formulated MPNPs exhibited a 92% efficiency in Ca^{2+} removal and can be effectively reused for up to four cycles. This efficiency is achieved through electrostatic interactions between the negatively charged polymer containing carboxylate groups and the hydrated Ca^{2+}, resulting in precipitation that prevents calcium carbonate scale formation.

Developing a rapid and user-friendly technique for detecting target compounds in practical environments remains a challenge. Polystyrene (PS) is considered a highly promising material due to its cost-effectiveness, versatility, and minimal negative environmental impact. PS is frequently used to create latex nanoparticles and is applied in various applications due to its substantial surface area, low density, and stability [33, 34]. The latex agglutination test quantifies a measurable aggregation phenomenon that can be easily observed with the naked eye. The particle supports are functionalized with active sites. When specific targets bind to these sites, particle clumping occurs, serving as an indicator of the presence of the target components or molecules. The extent of aggregation can be assessed visually by examining the area of the aggregate formations. Latex agglutination, using synthetic PS particles, has been extensively applied in various fields, including in vitro biomedical diagnosis, ecological risk assessment, and food contamination monitoring [35-38] thanks to its advantages, ease of use, cost-effectiveness, and high reliability. Furthermore, the reaction is visible, eliminating the need for specialized equipment or complex detection systems [39-41].

This research aims to develop functionalized polystyrene nanoparticles suitable for the rapid detection of the commonly used organophosphate, PBTC, in industrial water-cooling

systems and wastewater treatment processes using a latex agglutination assay. The research findings will be used to construct a map of aggregation domains as a function of PBTC concentration and pH, offering an effective approach for detecting PBTC concentration in unknown samples.

2. Materials and Methods

2.1 Materials

Styrene monomer (Janssen Chimica), 2,2'-azobis(2-amidinopropane) dihydrochloride (V50; >97%, Wako Chemical), 2-amino ethyl methacrylate hydrochloride (AEMH; Kodak chemicals), 2-phosphonobutane-1,2,4,-tricarboxylic acid (PBTC; >47% solution, Carl Roth), potassium antimony (III) oxide tartrate trihydrate (Carl Roth), ascorbic acid (Carl Roth), ammonium molybdate tetrahydrate (>99%, Sigma-Aldrich), sodium hydroxide (98%, Thermo Scientific), sulfuric acid (95%, VWR chemical BDH) were used as received. Deionized (DI) water was used throughout the study.

2.2 Methods

2.2.1 Preparation of cationic polystyrene latex particles

PS latexes bearing cationic amine groups were prepared following the procedure described elsewhere [42, 43]. Briefly, 20 g of styrene monomer and 2.5×10^{-3} g of AEMH functional monomer were added to a thermostat glass reactor containing 200 g deoxygenated water (DI water boiled under a nitrogen atmosphere). The mixture was continuously stirred at 300 rpm under a controlled temperature of 70 °C. After that, a small amount of initiator solution (V50, 0.32 g) was added to the mixture, and the polymerization was conducted for 20 h.

2.2.2 Characterization of cationic PS latex particles

The specimen was positioned inside a vacuum chamber with an accelerated voltage of 120 kV. The hydrodynamic size and size distribution of the prepared PS latex particles were measured using dynamic light scattering (DLS) with a ZetaSizer (nano series 3000MS, Malvern Instruments). The obtained polymer particles were diluted in 1 mM NaCl at a given pH. The reported size value was the average of three measurements. The morphology of the prepared

particles was examined using a scanning electron microscope (SEM, COXEM EM-30Plus). A droplet of the diluted latex particles was evaporated at room temperature, and the dried solid sample was gold-coated before analysis. Additionally, the synthesized particles were characterized using a transmission electron microscope (TEM, JEOL 1400 FLASH – Source LaB6). A droplet of diluted latex particles was deposited onto a formvar/carbon-coated copper 200-mesh grid. The specimen was positioned inside a vacuum chamber with an accelerated voltage of 120 kV.

2.2.3 Electrokinetic study of cationic PS latex particles

Electrophoretic mobility analysis was conducted on a ZetaSizer (nano series 3000HS, Malvern instrument). The measurements were operated using highly diluted dispersed latexes in 1 mM NaCl solution. The zeta potential deduced from the electrophoretic mobility of the PS latex particles was measured as a function of pH. The effect of PBTC concentrations (10-2,000 ppm) under different pH conditions (pH 3-11) on the electrokinetic behaviour was investigated. All measurements were conducted at 25 °C and interpreted as a direct study of the effective total surface charge density.

2.2.4 Adsorption of PBTC on cationic PS particles

A titration using a standard molybdate solution was employed to determine the amount of the adsorbed PBTC on the cationic PS particles. Molybdate reagent was prepared by combining; the following components: 100 mL of 2.5 M sulfuric acid solution, 10 mL of potassium antimony tartrate solution (dissolution of 0.28 g in 80 mL of distilled water and diluted to 100 mL), 30 mL of ammonium molybdate solution (prepared at 4% w/v), and 60 mL of ascorbic acid solution (1.76 g in 100 mL of DI water). After mixing, a light-yellow solution was obtained.

Adsorption kinetic of PBTC on PS latex particles

The synthesized PS latex particles (10 mg) were added to a series of centrifuge tubes, containing 10 mL of PBTC solution at an initial concentration of 1,000 ppm (with a fixed pH of 5). The samples were mixed for 0 – 120 min. At specific intervals during this period, the mixtures were centrifuged to separate the remaining phosphate phase. The supernatant of each sample was collected and filtered using a nylon microfilter (0.20 μm pore size). The post-treatment solution (5 mL) was transferred into a clean cuvette, and 0.8 mL of molybdate reagent

was added to the mixture for colorimetric measurements. The solution changed to a blue colour between 15-20 min. Subsequently, the solution's absorbance was recorded at 880 nm using an ultra-fast UV/Vis spectrometer (FLUOstar Omega). The batch experiment and sampling method were applied to obtain the adsorption kinetic of PBTC on the cationic PS latexes, as illustrated in Fig 1.

Adsorption rate of PBTC on PS particles

The adsorption isotherms were investigated in a similar manner to the kinetic experiments with 1 g/L of each solid-liquid latex. PBTC solutions at various concentrations ranging from 0 to 15,000 ppm were prepared at fixed pH values of 5, 6.5, and 11. The samples were gently mixed end-over-end at 35 rpm for 20 min. Subsequently, the mixtures were centrifuged at 7,500 rpm for 5 min, followed by filtration. The adsorption of the phosphate compound was examined using a colorimetric technique employing UV/Vis spectroscopy.

2.2.5 Latex agglutination assay for PBTC detection

The detection of PBTC at varied concentrations, from 0 to 2,000 ppm at a pH range from 3 to 11, was performed on a clean glass slide. Droplets of 10 μL of the synthesized PS latexes (containing 1 mg of particles) were deposited on the glass slide, forming separate circular domains. Subsequently, 30 μL of the prepared PBTC solutions at different concentrations were added and manually mixed for 15 seconds. The presence of agglutination phenomenon at each condition was observed by the naked eye, and photographs were taken.

3. Results and Discussion

3.1 Characterization of cationic PS latex particles

The PS latex particles were successfully prepared with a high polymerization conversion (~98%) using cationic 2-amino ethyl methacrylate hydrochloride (AEMH) as a functional monomer and 2,2'-azobis(2-amidinopropane) dihydrochloride (V50) as an initiator. The morphology of the prepared particles was examined by SEM and TEM, as shown in Figs 2(A and B). Spherical polymeric particles with smooth surfaces were generated. The synthesized particles exhibited uniform shape and morphology, as evidenced by the particle diameter of approximately 100±11 nm. Similar results were also observed from TEM analyses, where the average size of the functionalized PS colloidal particles, calculated from the statistical

distribution was 98±35 nm. A hydrodynamic particle size of 107.8±14 nm was observed (Fig 2C). It is important to note that the size determined from DLS is generally larger than that from TEM images [44], as the results from DLS represent the hydrodynamic diameter, which includes the hydrated layers on the colloidal surface. In contrast, TEM measures the diameter of the particles, under a dried state [45]. Nevertheless, high-quality size distribution curves of the colloidal dispersion were observed using the Contin analysis mode. This reflects the well-defined dispersion composed of homogeneous nano-spherical particles with a standard deviation of 27.92 nm relatively narrow size distribution [46].

3.2 Electrokinetic study

The zeta potential deduced from the electrophoretic mobility of the prepared PS latex particles was measured as a function of pH (with 1 mM NaCl solution), as summarized in Fig 3(A). The zeta potential exhibited positive values in the investigated pH range (3-12), indicating the cationic characteristic of the protonated amine groups on the particle's surfaces. The incorporated primary amine ($-NH_2$) groups from the functional monomer copolymerized with styrene onto the PS particles, were protonated, resulting in a high positive zeta potential at a pH lower than 10 [47, 48]. The zeta potential of the PS latex particles exhibited a rapid decrease in a strong basic environment (pH 11-12). The decrease of the zeta potential at high basic environments can be attributed to the deprotonation of ammonium ions to amine since the pH is above the pKa value of the applied 2-amino ethyl methacrylate hydrochloride, which is between 9 and 10. In addition, the decrease in the zeta potential at high pH can also be attributed to the possible condensation of hydroxyl groups on the particles' surface. However, the salinity variation is too low to induce the observed phenomenon. These results indicate that the synthesized products are suitable materials with high cationic properties, which should interact with the negatively charged compounds through favourable attractive electrostatic interactions [49, 50]. In addition, the electrophoretic mobility has been investigated as a function of electrolyte concentration, as presented in Fig 3(B). As expected, the electrophoretic mobility (in absolute value) decreases with increasing the salinity of the medium. This is in good agreement with the theory [51].

The surface charge density of the prepared particles was calculated using the following Helmholtz and Smoluchowski equation (Eq. 1):

$$\mu_e \approx \frac{\sigma}{\eta K} \qquad \text{Eq. 1}$$

where; μ_e is the electrophoretic mobility (μm·cm/ V·s); σ is the surface charge density (μC/cm^2); η is the dynamic viscosity of the continuous medium (Pa·s); and K (Greek kappa) is referred to as the inverse Debye length (k^{-1}) which is called the double layer thickness.

Since the surface potential is replaced by zeta potential (which is also an approximation approach), the surface charge density is not far from the presented approximated equation. In fact, the results data in which the surface charge density is reported as a function of surface potential, the deduced zeta potential was found to be in the limit of the linearity domain. Therefore, the equation used in this study is just for estimating the surface charge density rather than its exact determination [43]. It is noted that the surface charge density was calculated by considering the electrophoretic mobility, *i.e.*, the zeta potential of +46 mV, at a plateau value. The deduced surface charge density was 10 μC/cm^2 (where the specific surface area is 56 m^2/g). The value is comparable to those reported for PS latexes with amine or amidine groups prepared *via* the same polymerization process, which showed similar electrophoretic mobility tendencies [52].

3.3 pH effect on particles as a function of PBTC concentrations

The effect of adding the amine-functionalized colloidal latexes to PBTC stock solutions on the pH of the solutions was initially investigated, as shown in Fig 4. The addition of amine-functionalized PS latex particles did not affect the pH levels of the organophosphate solution, regardless of its concentrations. This confirms that the cationic characteristic of the polymer latex did not interfere with the controlled parameter in subsequent experiments. The zeta potential of amine-functionalized particles added to PBTC solutions was then examined as a function of pH, as summarized in Fig 5. As expected, the zeta potential was positive and slightly decreased due to the deprotonation of the primary amine and amidine groups from the AEMH copolymer and V50 initiator. Interestingly, the zeta potential remains positive until

reaching the vicinity of pH 10, which is close to the pKa of the primary amine [53]. Therefore, the zeta potential of latex particles was investigated as a function of both pH and PBTC concentration. The positive zeta potential of latex particles decreased with increasing PBTC concentrations, irrespective of their incubation pH. This decrease can be attributed to (i) the adsorption of negatively charged PBTC on the positively charged functionals (protonated amines and amidines) and (ii) the ionic strength effect of PBTC. Increasing the PBTC concentration increases the ionic strength of the incubation medium, leading to a reduction in the zeta potential.

PBTC has multiple acid functional groups (carboxylic acid), resulting in multiple pKa values (1.08±0.42, 3.99±0.21, 4.44±0.10, 4.99±0.14, and 8.59±0.50 for pKa 1-5, respectively) [6]. The pH is a significant factor that should be considered for controlling the number of negatively charged sites in the system. Furthermore, the zeta potential is highly influenced by the organophosphoric acid, which typically exhibits a positive charge in strongly acidic environments (pH 3-4), but immediately reduces in ionic strength with an increase in the PBTC dosage. The increase in the initial concentration results in more negative potential values, especially in basic conditions. The negative ion values likely originate from the three carboxylic groups and the orthophosphates, which are correlate with the amount of the reagent and the pKa of the solutions.

3.4 Adsorption behavior of PBTC on amine-functionalized PS latex particles

The adsorption efficiency of absorbents is commonly influenced by several factors, including electrostatic and other available interactions. For materials, the aggregation phenomenon typically occurs when the zeta potential reaches zero mV, which is defined as the isoelectric point and is often used as a reliable indicator of the pH range of instability [54, 55]. The surface charge represents the effective net and counter ions on the contact layer and reflects the ability of the amino-functional group to interact with negative counter ions. The observed changes in this study are associated with the adsorption of negative ions from PBTC structures in the solutions. Even though the ionic strength is the key determining factor for aggregation-dispersion according to DLVO theory, in this study, the salinity in the PBTC solution to be analyzed the critical coagulation concentration (CCC) is low (below 1 mM NaCl, since pure water is generally used in cooling systems). Therefore, the PBTC concentration to be detected is below the CCC of the applied latex particles.

Adsorption kinetics of PS latex particles

The adsorption kinetics of PBTC on the functionalized PS latex particles was investigated by measuring the adsorption capacity as a function of incubation time, as shown in Fig 6. The sorption event rapidly occurred during the first 3 min of the experiment. As the ionic strength of the functionalized PS particles at the studied pH (pH 5) is positive and the target PBTC compound contains anionic species, it appears that the primary mechanism of this adsorption is induced by electrostatic attraction. However, after 10 min, however, there is no significant increase in the adsorption capacity, indicating an equilibrium state. The observed relatively short equilibrium time is consistent with prior studies, where the strong interaction from oppositely-charged molecules/groups on the particle surfaces led to a fast equilibrium within 10-20 min [56, 57]. These results confirm the interactions between the protonated amine groups and the available active anions in the PBTC structures.

Adsorption isotherms of PBTC as a function of pH and initial PBTC concentration

The adsorption isotherms of the organophosphate reagent on the PS latex particles's surfaces at different pH conditions are compared in Fig 7. The equilibrium adsorption capacity of the particles as a function of residual PBTC concentration is compared at different pH conditions. The equilibrium adsorption capacity increased with the residual PBTC concentration from 0 to 9000 ppm, due to higher contents of available negatively charged species in the system. The value reached a plateau value of around 0.011-0.012 μmol/cm^2, reflecting the maximum adsorption capacity. This indicates that the essential factor affecting the adsorption capacity is the concentration of PBTC, as its -COOH and -PO_3H_2 groups undergo ionization *via* deprotonation. The increase in the initial concentration of PBTC leads to higher adsorption capacity on the adsorbent surface, due to the electrostatic force between the protonated functionalized nanoparticles and negative PBTC in the media [58, 59]. Similar results were also observed at all pH conditions. Although the effect of pH on the adsorption capacity has not been widely studied, the results on PBTC adsorption as a function of pH on ZrFeZn adsorbent, which carries positive charges have been reported [60]. The authors reported a similar tendency, where the adsorption of PBTC occurred at pH range > 5 and did not significantly change with increased pH values. It is noted that upon closer examination of our results, the PBTC adsorption capacity was slightly reduced in the solution with high pH (> 10). This is likely because the charge on the PS adsorbent particles may shift in the negative direction with increasing solution pH due to a

lower degree of protonation. Even though the critical coagulation concentration (CCC) can be estimated from the surface charge density and macroscopically examined for such latex particles, also the CCC domain has been estimated from quick latex particle agglutination as a function of NaCl and found to be in between 5 x 10-2 to 10-1 M. In this work, the salinity of the PBTC solution to be analyzed is very low (below 1mM NaCl, since pure water is generally used in cooling systems). Thus, the PBTC concentration to be detected is below the CCC of the used latex particles.

Considering that the surface charge density of latex particles is related to the number of mobile charges carried per unit area, the adsorption experiments were performed under a controlled number of particles that carry positive charges to investigate the adsorption mechanism. The proton equivalents were calculated to reveal a suitable mechanism for the adsorption features. The total surface charge was estimated by equation (Eq. 2);

$$\sigma \approx \frac{e_p \phi_p}{6} \times n_{eq} \times N_A \times C_e^{-} \quad \text{(Eq. 2)}$$

where; σ is the surface charge density (μC/cm^2) deduced from zeta potential as discussed above; $e_p$is the solid density (g/cm^3); ϕ_p is particle diameter (nm); n_{eq} is the number of protons equivalent (μmole/cm^2); N_A is the Avogadro's number (6.022×10^{23} mol^{-1}); and C_e^{-} is the electric charge (1.602×10^{-19} C, coulomb).

The n_{eq} value of the original PS latex particles, calculated from Eq. 2 was 1.04×10^{-4} μmole/cm^2. From the adsorption experiments, the total adsorption amount of PBTC on the positively charged particles is also expressed in μmole/cm^2. The calculated values as a function of pH are summarized in Fig 8. The PBTC adsorption capacity is significantly higher than the available positive sites for adsorption. This indicated that the available protonated amino groups on the surface completely interact with an equimolar amount of negative PBTC ions through electrostatic interaction. Additionally, the presence of a large excess of adsorbed PBTC is likely due to hydrogen bonding between carboxylic acids and -NH_2 acceptor [61].

3.5 Latex aggregation assay

From the adsorption results, the observed aggregation of the latex particles is likely correlated with the incubation pH and PBTC concentration at a given latex particle content. However, in this study, however, specific attention is dedicated to the rapid agglutination only to detect the PBTC concentration range of unknown aqueous samples, as shown in Fig 9. As evidenced from the experiments (agglutination *vs.* pH and PBTC concentrations), two macroscopic aggregation domains were well distinguished, *i.e.*, stable (no macroscopic aggregation) and unstable domain. Below 50 ppm of PBTC, only a stable domain was observed, irrespective of pH. This is due to the low PBTC adsorption amounts. In contrast, when the PBTC concentration was above 50 ppm, the presence of the aggregation domain was dependent on both PBTC concentration and pH. At 100 ppm PBTC, the aggregation appeared at pH 11, while at 500 and 1000 to 2000 ppm PBTC, this occurred at pH > 6.5, and > 5, respectively. As discussed above, the amount of adsorbed PBTC increases with increasing PBTC initial concentration. In addition, increasing the incubation pH above the average pKa of PBTC also leads to an increase in adsorption capacity. The excess adsorption of PBTC, in turn, causes surface charge screening, leading to lower surface charge density and low colloidal stability of the dispersion. Therefore, aggregation of the latex particles is observed. This phenomenon can also be deduced from zeta potential measurement as a function of both pH and PBTC concentration. The results, as reported in Fig 10, quantitatively indicate the macroscopic phenomenon observed in Fig 9. At low PBTC concentration (<500 ppm) and acidic pH (<5), PBTC dissociation is low. Consequently, low PBTC adsorption occurred, and no zero-zeta potential domain was observed. By increasing the PBTC concentration and the incubation pH, the aggregation phenomenon occurred in the zero-zeta potential range. This is mainly governed by charge-charge electrostatic interactions. This phenomenon can be applied in rapidly detecting the PBTC concentration range of unknown aqueous solutions.

In the practical detection of PBTC concentration, an unknown solution is sampled, and its pH is measured. PBTC or PBTC derivatives are employed in a low concentration range. The major competitive compounds that possess similar functional groups may be other phosphate species. The experiments were conducted in a phosphate buffer solution, which accounts for a high concentration of possible competitors. Then, the agglutination test is performed by mixing the solution and the synthesized PS latexes at a given ratio. After 1 min, the aggregation domain state (stable/unstable) is evaluated. For example, if the unknown sample (measured at pH 7)

shows macroscopic aggregation after mixing, this means that the concentration range of PBTC is higher than 500 ppm. The sample's pH is then adjusted to a more acidic value until a stable domain (no macroscopic aggregation) is observed. The concentration of PBTC in the unknown solution is therefore identified. However, if there is still macroscopic aggregation after adjusting the pH to strong acidic conditions, dilution of the unknown sample is required, and the diluted solution is subjected to the same procedure. In contrast, if the macroscopic aggregation is not detected at the first test, the pH of the solution is adjusted to more basic conditions until aggregation occurs. However, if no macroscopic aggregation is observed after reaching very strong basic conditions, it may be due to an excessively low PBTC concentration, and the unknown solution needs to go through a concentrating process (e.g., by evaporation method). The developed latex agglutination assay is facile and does not require special skills or equipment for operation. The technique is applicable for monitoring a wide range of PBTC concentrations and has high potential for practical use in various fields, especially in industrial water-cooling systems, wastewater treatment processes, and toxic compound monitoring.

4. Conclusions

A process for qualitative and quantitative detection of organophosphate (PBTC) has been successfully developed using a simple latex agglutination assay. Positively charged PS latex particles, prepared through emulsifier-free emulsion polymerization, serve as the adsorbent. The obtained amine-functionalized PS particles exhibit monodispersity with an average diameter of 100±11 nm. The incorporation of primary amine from the AEMH comonomer results in a high positive zeta potential value (+46 mV) at a pH below 10. In addition, the behaviour of the nanoparticles under different conditions (pH and PBTC concentration) was investigated. The zeta potential decreased with the rising pH and PBTC concentration, especially at high concentrations. This rapid modification of the surface charge is attributed to an overload of negative charge values in the system. Furthermore, increasing the PBTC dosage led to a decrease in the zeta potential of the particles, eventually reaching equilibrium under basic conditions, indicating that suitable positive sites were completely occupied. Adsorption kinetics and isotherms of PBTC on the material's surface were examined to determine the adsorption capacity and mechanism using a colorimetric method. The quantitative results indicated that increasing

PBTC content in the aqueous medium improves the particle's adsorption capacity. In addition, increasing the pH value generated more negative ions from the deprotonation of the acid groups, leading to increased adsorption capacity. The results suggest that the electrostatic interactions and hydrogen bonding between the positively charged layer on the particle's surface and negatively charged organophosphate molecules drive the latex aggregation mechanism. This mechanism can be effectively employed for the rapid detection of PBTC concentration. Positively charged PS particles offer promising opportunities for the practical monitoring of phosphate additives in a water medium, offering a simple process, fast detection, low cost, and reduced chemical and equipment. In the case of mixtures, the PBTC detection may be impacted depending on the nature of the compounds present in the system. However, without dedicated experiments, it is not possible to affirm to which extent the detection will be impacted at this stage.

5. Acknowledgments

This study is supported by the NSRF via the Program Management Unit for Human Resources & Institutional Development, Research, and Innovation (grant number B16F640084), the Center of Excellence in Functional Advanced Materials Engineering (CoE FAME), Thammasat University. The scholarship support from the National Science and Technology Development Agency (NSTDA)/Thammasat University, Thailand, through the Excellent Research Graduate Scholarship and the Excellent Thai Students (ETS) from Sirindhorn International Institute of Technology (SIIT), Thammasat University, and the Franco-Thai Scholarship Program 2023 from France Embassy in Thailand to J.J. is gratefully acknowledged.

6. References

1. Zhang, B., et al., *Testing the formation of Ca–phosphonate precipitates and evaluating the anionic polymers as Ca–phosphonate precipitates and CaCO3 scale inhibitor in simulated cooling water*. Corrosion Science, 2010. **52**(12): p. 3883-3890.

2. Zhang, X., et al., *Rapid determination of aminotris(methylenephosphonic acid) in water by ultraviolet photooxidation.* Instrumentation Science & Technology, 2016. **45**(4): p. 459-468.
3. Xu, J., et al., *Development of an online analyzer for determination of total phosphorus in industrial circulating cooling water with UV photooxidation digestion and spectrophotometric detection.* Talanta, 2019. **201**: p. 74-81.
4. Li, X., et al., *Effect of six kinds of scale inhibitors on calcium carbonate precipitation in high salinity wastewater at high temperatures.* J Environ Sci (China), 2015. **29**: p. 124-30.
5. Huang, Y., et al., *Highly selective uranium adsorption on 2-phosphonobutane-1,2,4-tricarboxylic acid-decorated chitosan-coated magnetic silica nanoparticles.* Chemical Engineering Journal, 2020. **388**.
6. Kretzschmar, J., et al., *2-Phosphonobutane-1,2,4,-Tricarboxylic Acid (PBTC): pH-Dependent Behavior Studied by Means of Multinuclear NMR Spectroscopy.* Molecules, 2022. **27**(13).
7. Demadis, K.D. and P. Lykoudis, *Chemistry of Organophosphonate Scale Growth lnhibitors: 3. Physicochemical Aspects of 2-Phosphonobutane-1,2,4-Tricarboxylate (PBTC) And Its Effect on C<small.letters>a</small.letters>CO₃ Crystal Growth.* Bioinorganic Chemistry and Applications, 2005. **3**: p. 546865.
8. Jonasson, R.G., et al., *Effect of phosphonate inhibitors on calcite nucleation kinetics as a function of temperature using light scattering in an autoclave.* Chemical Geology, 1996. **132**(1): p. 215-225.
9. Hussein, A. and H. Sabry, *Factors affecting phosphonate measurement by inductively coupled plasma optical emission spectroscopy (ICP-OES) in oilfield produced waters.* International Journal of Environmental Analytical Chemistry, 2019. **100**: p. 1-18.
10. Al Nasser, W.N., et al., *Inline monitoring the effect of chemical inhibitor on the calcium carbonate precipitation and agglomeration.* Chemical Engineering Research and Design, 2011. **89**(5): p. 500-511.
11. Jaworska, J., et al., *Environmental risk assessment of phosphonates, used in domestic laundry and cleaning agents in the Netherlands.* Chemosphere, 2002. **47**(6): p. 655-665.

12. Studnik, H., et al., *Amino polyphosphonates – chemical features and practical uses, environmental durability and biodegradation.* New Biotechnology, 2015. **32**(1): p. 1-6.
13. Bunce, J.T., et al., *A Review of Phosphorus Removal Technologies and Their Applicability to Small-Scale Domestic Wastewater Treatment Systems.* Frontiers in Environmental Science, 2018. **6**.
14. Bricker, S.B., et al., *Effects of nutrient enrichment in the nation's estuaries: A decade of change.* Harmful Algae, 2008. **8**(1): p. 21-32.
15. Li, J., et al., *Highly Efficient Removal of Nitrate and Phosphate to Control Eutrophication by the Dielectrophoresis-Assisted Adsorption Method.* Int J Environ Res Public Health, 2022. **19**(3).
16. Dhaka, S., et al., *Metal–organic frameworks (MOFs) for the removal of emerging contaminants from aquatic environments.* Coordination Chemistry Reviews, 2019. **380**: p. 330-352.
17. Guo, Z.X., Q. Cai, and Z. Yang, *Determination of glyphosate and phosphate in water by ion chromatography--inductively coupled plasma mass spectrometry detection.* J Chromatogr A, 2005. **1100**(2): p. 160-7.
18. Cheng, H., et al., *Enzymatic Behavior Regulation-Based Colorimetric and Electrochemiluminescence Sensing of Phosphate Using the Cobalt Oxyhydroxide Nanosheet.* Analytical Chemistry, 2021. **93**(17): p. 6770-6778.
19. Moumen, E., L. Bazzi, and S. El Hankari, *Metal-organic frameworks and their composites for the adsorption and sensing of phosphate.* Coordination Chemistry Reviews, 2022. **455**.
20. Forano, C., H. Farhat, and C. Mousty, *Recent trends in electrochemical detection of phosphate in actual waters.* Current Opinion in Electrochemistry, 2018. **11**: p. 55-61.
21. Bazan-Wozniak, A., et al., *Adsorption of Organic Compounds on Adsorbents Obtained with the Use of Microwave Heating.* Materials (Basel), 2022. **15**(16).
22. De Gisi, S., et al., *Characteristics and adsorption capacities of low-cost sorbents for wastewater treatment: A review.* Sustainable Materials and Technologies, 2016. **9**: p. 10-40.
23. Zanini, M., et al., *Universal emulsion stabilization from the arrested adsorption of rough particles at liquid-liquid interfaces.* Nat Commun, 2017. **8**: p. 15701.

24. Tao, J. and A.M. Rappe, *Physical adsorption: theory of van der Waals interactions between particles and clean surfaces.* Phys Rev Lett, 2014. **112**(10): p. 106101.
25. Hou, L., Q. Liang, and F. Wang, *Mechanisms that control the adsorption-desorption behavior of phosphate on magnetite nanoparticles: the role of particle size and surface chemistry characteristics.* RSC Adv, 2020. **10**(4): p. 2378-2388.
26. Bernal, V., et al. *Effect of Solution pH on the Adsorption of Paracetamol on Chemically Modified Activated Carbons*. Molecules, 2017. **22**, DOI: 10.3390/molecules22071032.
27. De Oliveira, T., et al., *Adsorption of diclofenac onto organoclays: Effects of surfactant and environmental (pH and temperature) conditions.* Journal of Hazardous Materials, 2017. **323**: p. 558-566.
28. Bernal, V., et al. *Mechanisms of Methylparaben Adsorption onto Activated Carbons: Removal Tests Supported by a Calorimetric Study of the Adsorbent–Adsorbate Interactions*. Molecules, 2019. **24**, DOI: 10.3390/molecules24030413.
29. Wang, H., Z. Chai, and D. Wang, *Influence of anions on the adsorption of uranyl on hydroxylated α-SiO2(001): A first-principles study.* Green Energy & Environment, 2017. **2**(1): p. 30-41.
30. Cheng, S., et al., *Enhanced adsorption performance of UiO-66 via modification with functional groups and integration into hydrogels.* Environmental Research, 2022. **212**: p. 113354.
31. Samal, S.K., et al., *Cationic polymers and their therapeutic potential.* Chem Soc Rev, 2012. **41**(21): p. 7147-94.
32. Kaewsaneha, C., et al., *Self-assembly of amphiphilic poly(styrene-b-acrylic acid) on magnetic latex particles and their application as a reusable scale inhibitor.* RSC Adv, 2020. **10**(67): p. 41187-41196.
33. Loos, C., et al., *Functionalized polystyrene nanoparticles as a platform for studying bio-nano interactions.* Beilstein J Nanotechnol, 2014. **5**: p. 2403-12.
34. Neves Libório De Avila, J., et al., *Polystyrene nanoparticles as surfactant carriers for enhanced oil recovery.* Journal of Applied Polymer Science, 2016. **133**(32).
35. Cruz, C.J.G., et al., *Malarial Antibody Detection with an Engineered Yeast Agglutination Assay.* ACS Synthetic Biology, 2022. **11**(9): p. 2938-2946.

36. Alamuri, A., et al., *Expression of Recombinant Leptospiral Surface Lipoprotein-Lsa27 in E. coli and Its Evaluation for Serodiagnosis of Bovine Leptospirosis by Latex Agglutination Test.* Molecular Biotechnology, 2020. **62**(11): p. 598-610.
37. Wang, J., et al., *Aggregation and stability of sulfate-modified polystyrene nanoplastics in synthetic and natural waters.* Environ Pollut, 2021. **268**(Pt A): p. 114240.
38. Ramarao, N., et al., *Advanced Methods for Detection of Bacillus cereus and Its Pathogenic Factors.* Sensors (Basel), 2020. **20**(9).
39. Esmail, S., et al., *Rapid and accurate agglutination-based testing for SARS-CoV-2 antibodies.* Cell Rep Methods, 2021. **1**(2): p. 100011.
40. Saringer, S., et al., *Papain Adsorption on Latex Particles: Charging, Aggregation, and Enzymatic Activity.* J Phys Chem B, 2019. **123**(46): p. 9984-9991.
41. Sethuraman, A. and G. Belfort, *Protein Structural Perturbation and Aggregation on Homogeneous Surfaces.* Biophysical Journal, 2005. **88**(2): p. 1322-1333.
42. Ganachaud, F., et al., *Emulsifier-free emulsion copolymerization of styrene with two different amino-containing cationic monomers. I. Kinetic studies.* Journal of Applied Polymer Science, 1997. **65**: p. 2315-2330.
43. Sauzedde, F., et al., *Emulsifier-free emulsion copolymerization of styrene with two different amino-containing monomers: II. Surface and colloidal characterization.* Journal of Applied Polymer Science, 1997. **65**(12): p. 2331-2342.
44. Zou, H., J. Liu, and X. Wang, *Surfactant-free emulsion copolymerization of styrene and a cationic comonomer with two positively charged groups.* Colloid and Polymer Science, 2019. **297**(7): p. 1133-1142.
45. Levy, I., et al., *Bioactive magnetic near Infra-Red fluorescent core-shell iron oxide/human serum albumin nanoparticles for controlled release of growth factors for augmentation of human mesenchymal stem cell growth and differentiation.* J Nanobiotechnology, 2015. **13**: p. 34.
46. Ouyang, Y., et al., *Highly monodisperse microporous polymeric and carbonaceous nanospheres with multifunctional properties.* Sci Rep, 2013. **3**: p. 1430.
47. Thompson, K.L., E.S. Read, and S.P. Armes, *Chemical degradation of poly(2-aminoethyl methacrylate).* Polymer Degradation and Stability, 2008. **93**(8): p. 1460-1466.

48. Liang, X., et al., *Efficient synthesis of high solid content emulsions of AIE polymeric nanoparticles with tunable brightness and surface functionalization through miniemulsion polymerization.* Dyes and Pigments, 2019. **163**: p. 371-380.
49. Duracher, D., et al., *Cationic amino-containing N -isopropyl- acrylamide-styrene copolymer particles: 2-surface and colloidal characteristics.* Colloid & Polymer Science, 1998. **276**(10): p. 920-929.
50. Mirnik, M. *Electrostatic and chemical interactions of ions in electrolytes and in ionic-point-charge double layers*. in *Trends in Colloid and Interface Science XIII*. 1999. Berlin, Heidelberg: Springer Berlin Heidelberg.
51. Moraila-Martinez, C.L., et al., *An experimental/theoretical method to measure the capacitive compactness of an aqueous electrolyte surrounding a spherical charged colloid.* J Chem Phys, 2018. **148**(15): p. 154703.
52. Chaix, C., et al., *Surface functionalization of oil-in-water nanoemulsion with a reactive copolymer: colloidal characterization and peptide immobilization.* Colloids and Surfaces B: Biointerfaces, 2003. **29**(1): p. 39-52.
53. Debons, N., et al., *Mapping amine functions at nanosurfaces using colloidal gold conjugation.* Applied Surface Science, 2021. **566**.
54. Meng, X., et al., *Application of Iron Oxide as a pH-dependent Indicator for Improving the Nutritional Quality*. Clinical Nutrition Research, 2016. **5**: p. 172.
55. Romdhane, A., et al., *Effect of pH and ionic strength on the electrical charge and particle size distribution of starch nanocrystal suspensions.* Starch - Stärke, 2015. **67**(3-4): p. 319-327.
56. Duracher, D., et al., *Adsorption of bovine serum albumin protein onto amino-containing thermosensitive core-shell latexes.* Polymer International, 2004. **53**(5): p. 618-626.
57. Polpanich, D., P. Tangboriboonrat, and A. Elaissari, *Preparation and agglutination of immuno-nanolatex for malaria diagnosis.* J Biomed Nanotechnol, 2009. **5**(5): p. 486-92.
58. Salvadó, V., M.L.s. Escoda, and F. de la Torre, *A study of the complex formation between trivalent ions (Al3+, Fe3+) and 2-phosphonobutane-1,2,4-tricarboxylic acid and their industrial applications.* Polyhedron, 1999. **18**(25): p. 3275-3280.

59. Kornev, V.I., T.N. Kropacheva, and U.V. Sorokina, *Coordination compounds of oxovanadium(IV) with organophosphonic complexones in aqueous solutions.* Russian Journal of Inorganic Chemistry, 2015. **60**(3): p. 403-408.
60. Rott, E., et al., *Removal of phosphonates from synthetic and industrial wastewater with reusable magnetic adsorbent particles.* Water Res, 2018. **145**: p. 608-617.
61. Bovone, G., et al., *Engineering Hydrogel Adhesion for Biomedical Applications via Chemical Design of the Junction.* ACS Biomater Sci Eng, 2021. **7**(9): p. 4048-4076.

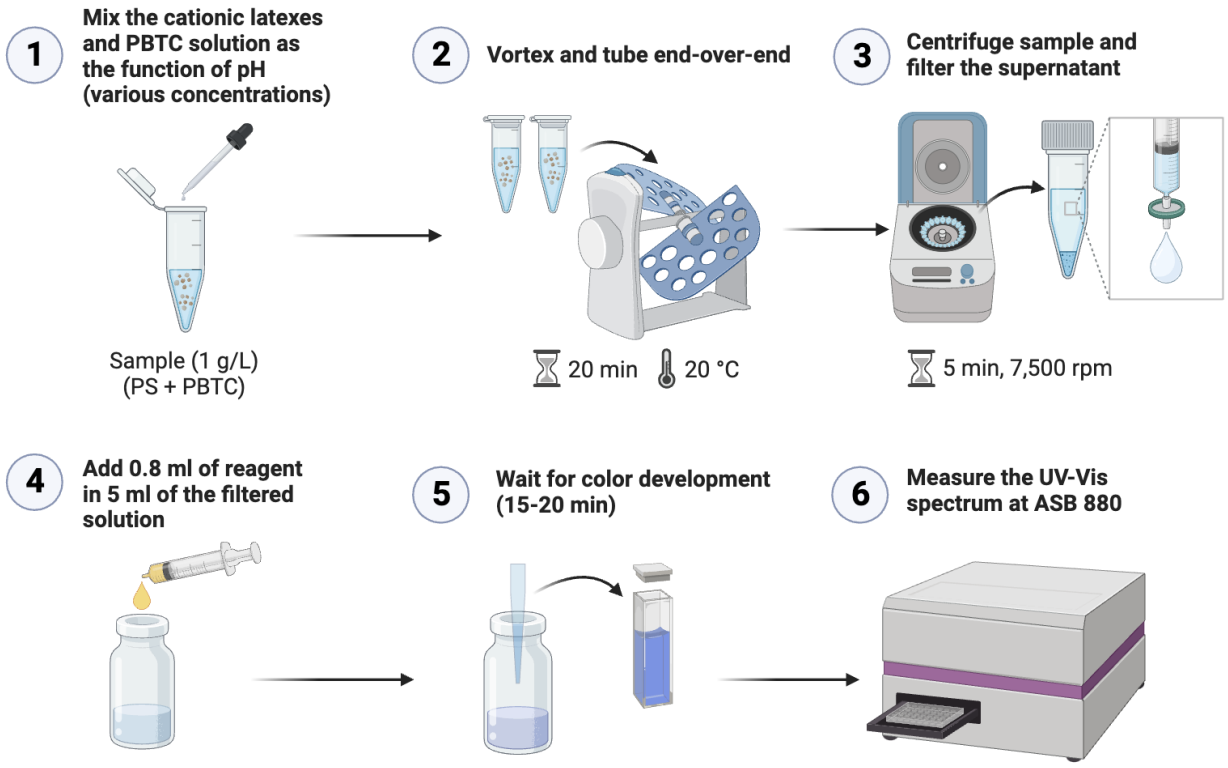

Fig 1. The adsorption process of PBTC on the cationic PS latex particles and the colorimetric determination

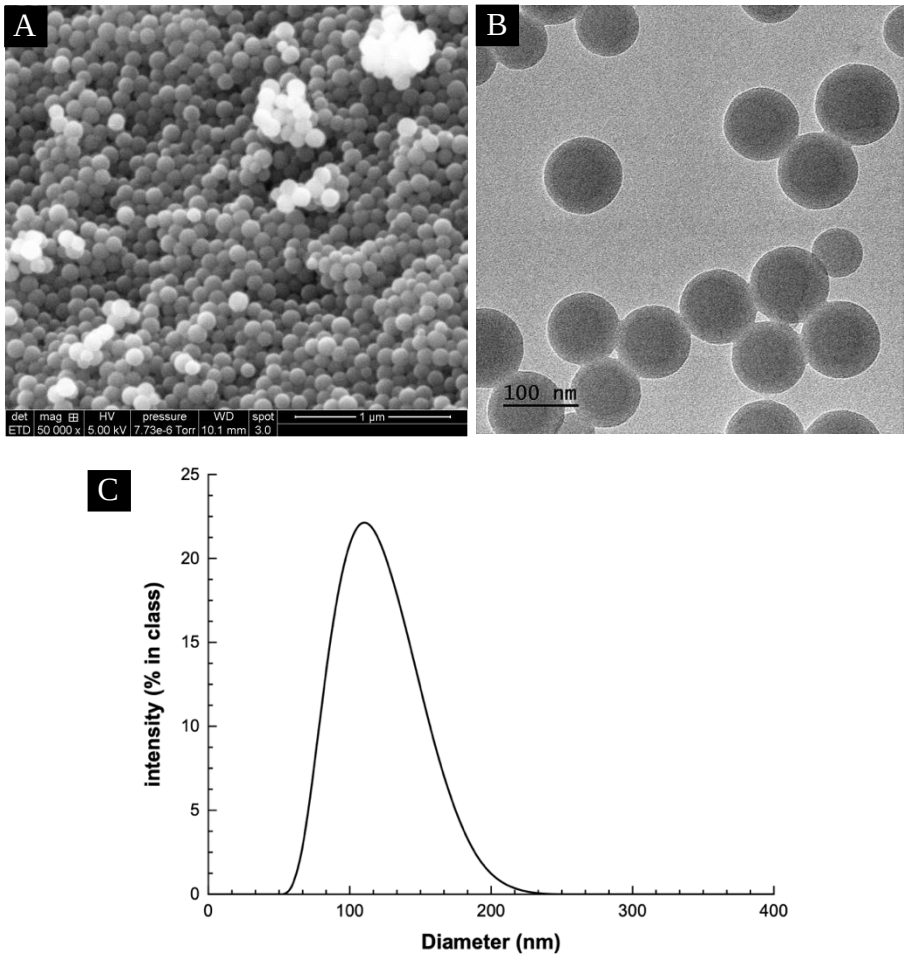

Fig 2. SEM (A) and TEM (B) images and hydrodynamic size (C) of the prepared cationic PS latex particles

(A)

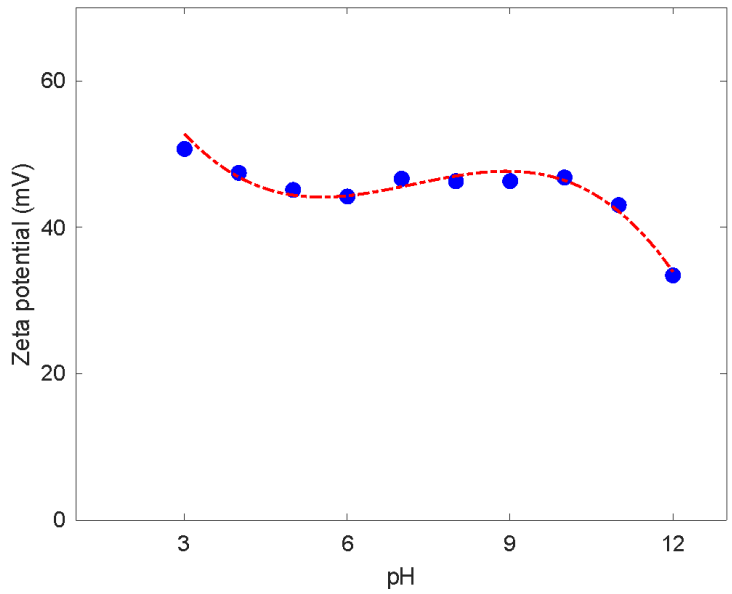
Zeta potential (mV)
60
40
20
0
3
6
9
12
pH

(B)

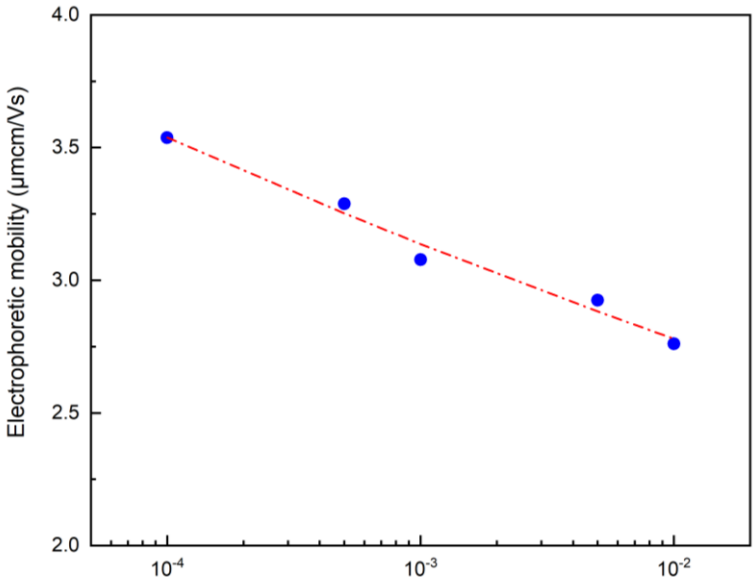
Electrophoretic mobility (μmcm/Vs)
4.0
3.5
3.0
2.5
2.0
10-4
10-3
10-2

Fig 3. (A) Zeta potential of the prepared cationic PS latex particles as a function of pH and (B) Impact of electrolyte concentration on the electrophoretic mobility of PS latex particles

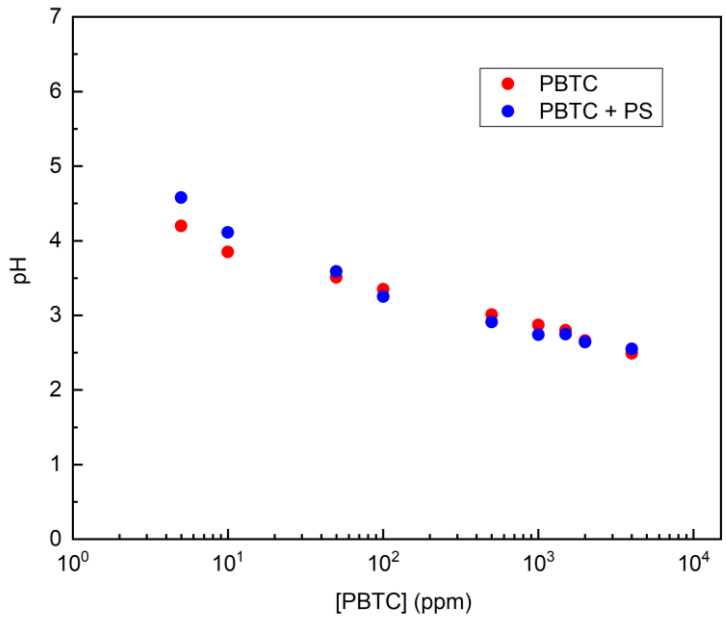

Fig 4. Effect of adding PS latex particles on the pH of PBTC solutions at different concentrations

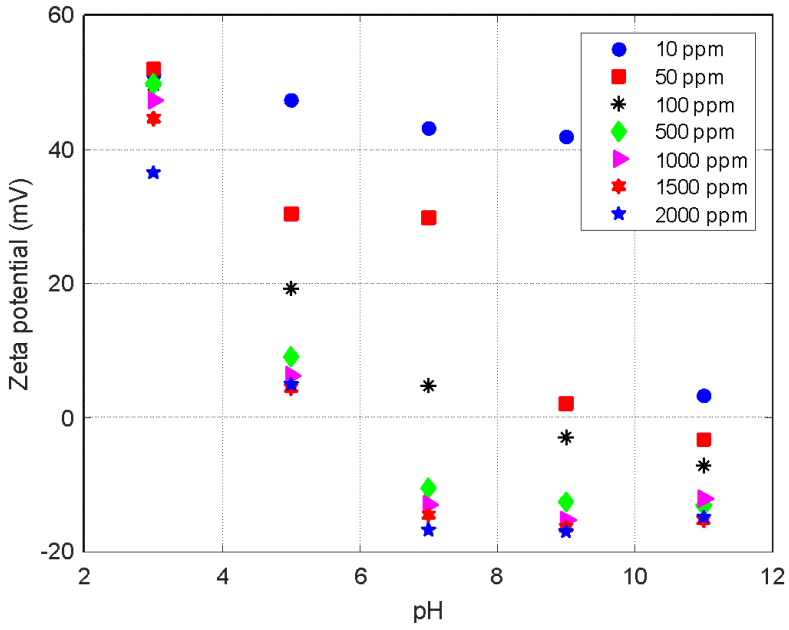

Fig 5. Zeta potential of cationic PS latex particles added in PBTC solutions as a function of PBTC concentrations at specific pH between 3-11

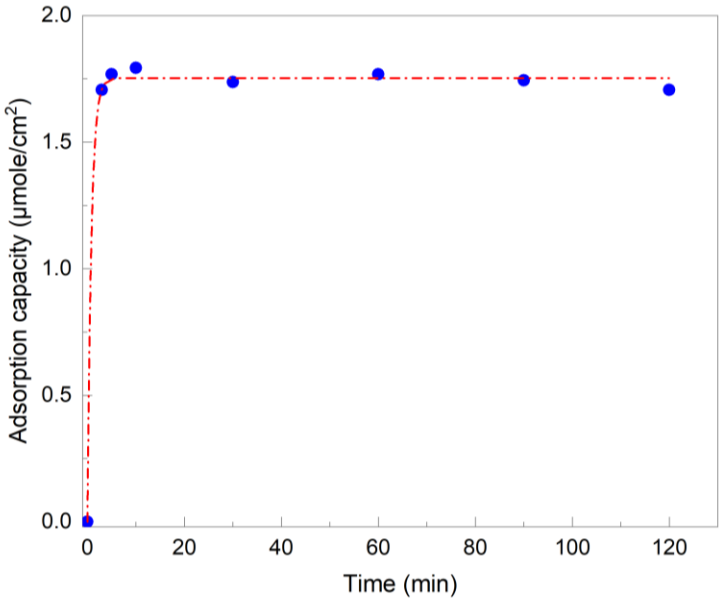

Fig 6. The adsorption kinetics of PBTC on the PS latex particle's surfaces at an initial PBTC concentration of 1000 ppm and pH 5

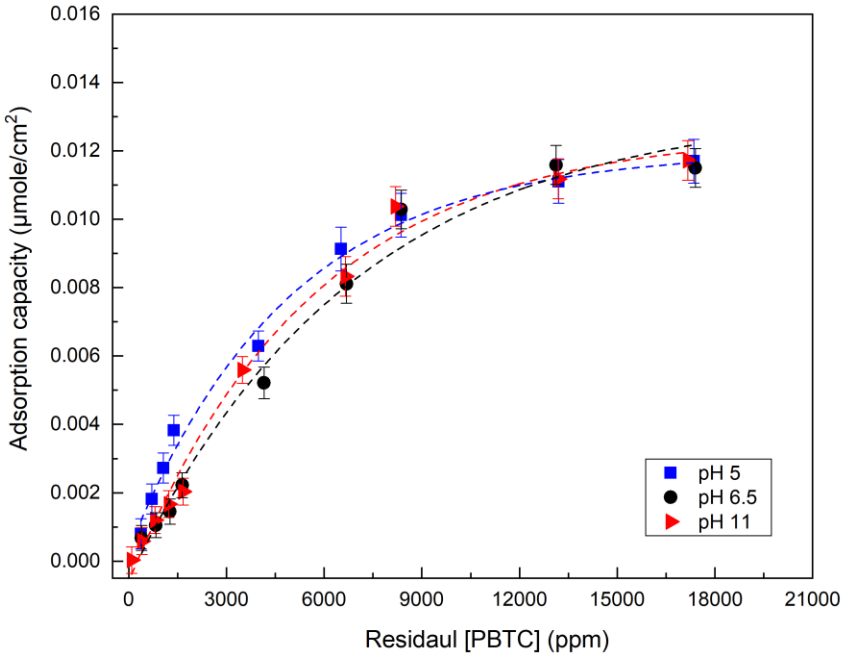

Fig 7. The adsorption isotherm of PBTC on the PS latex particle's surface at different pH conditions

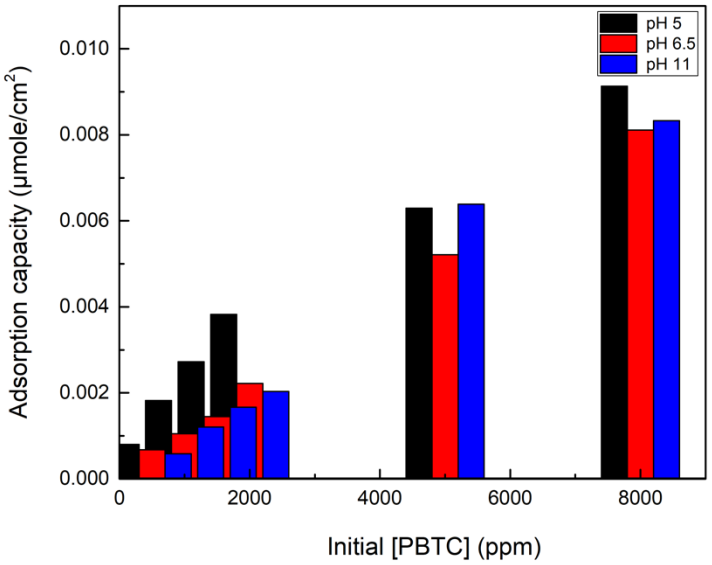

Fig 8. The adsorption capacity of the anionic-charged PBTC on the particle's surface at different pH and the initial PBTC concentrations

729

730

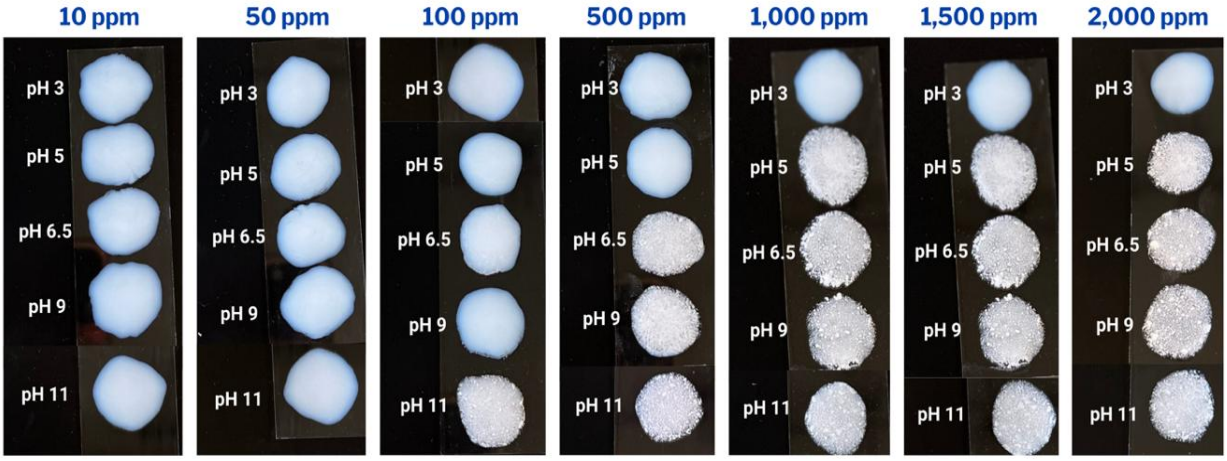

731

732 Fig 9. Latex aggregation phenomenon for PBTC detection as a function of pH and PBTC

733 concentration

734

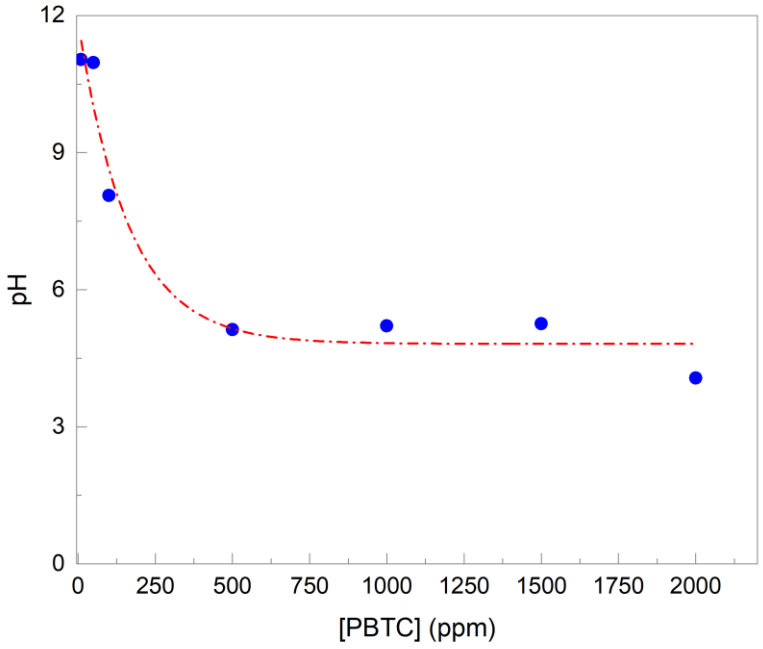

735

736 Fig 10. The relationship between pH and PBTC concentration at zero-zeta potential points